1963-04-01

Radar-Ray Refraction Associated with Horizontal Variations in the Refractivity

Martin, F.L.; Wright, F.E.

Journal of Geophysical Research Vol. 68, No. 7 April 1, 1963 p. 1861-1869
https://hdl.handle.net/10945/50457

Radar-Ray Refraction Associated with Horizontal Variations in the Refractivity

F. L. MARTIN AND F. E. WRIGHT[1]

U. S. Naval Postgraduate School, Monterey, California

Abstract. The relative bending effects on a radio ray of the horizontal and vertical gradient of refractivity are investigated. With the use of ray-curvature formulas developed by Wong, convenient differential equations governing the three-dimensional ray path are derived. It is also shown that the ratio of 'horizontal to vertical' bending effects is maximum when the ray is propagated in the vertical plane containing the horizontal gradient of refractivity. In a two-dimensional example, computations of path height as a function of horizontal distance are obtained by numerical integration. For this purpose, a regional space-time averaged exponential model drawn from climatological studies of Bean and Thayer has been used. Even though this smoothed model and an extreme version of it derived synthetically by increasing the horizontal gradient everywhere by a factor of 10 have comparatively strong horizontal gradients, the 'horizontal bending' effect is virtually negligible. It is not implied, however, that this conclusion is necessarily applicable to an atmosphere exhibiting small-scale fluctuations in the refractivity pattern. The ray paths corresponding to the nonhomogeneous model are significantly different from those in a horizontally uniform atmosphere. The problem of replacing a nonhomogeneous model by an equivalent horizontally uniform one is also investigated. The choice of the best uniform atmosphere depends upon minimizing the rms height error over a designated horizontal path length, and this in turn requires the specification of several ray-propagation parameters in addition to the distribution of refractivity.

1. *Introduction.* In tracing the ray path of high-frequency radio waves, we frequently use a model atmosphere in which the refractive index n is a function of height alone. *Bean and Thayer* [1959] and others have proposed models having the property that the refractivity $N = (n - 1) \times 10^6$ decreases exponentially with height above the surface. In such models, N is respresentable in terms of climatological data in the form

$$N = N_s \exp(-c_e z) \quad (1)$$

where N_s is the surface mean value of the refractivity, z is the height above the earth's surface, and c_e is the *decay factor* which depends upon N_s.

The values of N and N_s are determined from meteorological data by use of the Smith-Weintraub equation

$$N = 77.6(p/T) + 3.73 \times 10^5(e/T^2) \quad (2)$$

where p is the atmospheric pressure in millibars, T is the absolute temperature, and e is the water-vapor pressure in millibars.

[1] Now at Naval Security Group Activity, Fort George G. Meade, Maryland.

The primary usefulness of model atmospheres is to approximate closely the average radio-ray refraction that is based on climatic conditions. Starting with the original '4/3-earth model,' many improvements have been made to achieve progressively closer approximations to average ray bending. No effective way has yet been devised to include horizontal variations in these refractivity models, however. In order that ray paths may be computed by high-speed digital computers, it is frequently convenient to assume that the refractivity is horizontally stratified with respect to the earth's surface, thus allowing no horizontal variation of refractivity.

It is well known that Snell's law in the plan-stratified case follows from *Fermat's principle* of the minimum-time ray path [*Kerr*, 1951]. When the refractivity is horizontally uniform with respect to the spherical surface of the earth, Snell's law may be generalized to the form

$$n(z + a) \cos \theta = n_0(z_0 + a) \cos \theta_0 \quad (3)$$

where θ is the ray-elevation angle at any height z along the ray trajectory and a is the radius of the earth. The subscript zero on the right side of (3) indicates known initial conditions along

the ray. Using (3), it is possible to show [*Smart*, 1931] that the differential bending $d\tau$ along the ray path (considered positive in the case of downward bending) is given by

$$d\tau = -(dn/n) \cot \theta \tag{4}$$

The total bending $\tau_{1,2}$ between two fixed points is then given by

$$\tau_{1,2} = -\int_{n_1}^{n_2} \frac{\cot \theta}{n}\, dn \tag{5}$$

Since effects of horizontal variations in refractivity are to be considered in this paper, a more general ray-tracing method will be applied. We draw upon results given by *Kerr* [1951, pp. 43–44] for the special case in which the gradient of n lies in the vertical plane:

$$\frac{d\tau}{ds} = \frac{\nabla n \cdot \mathbf{u}}{n} = \frac{|\nabla n| \sin \gamma}{n} \tag{6}$$

Here $d\tau/ds$ is the two-dimensional[2] curvature K at any point of the ray, $\mathbf{u}$ is the *downward-directed* unit vector normal to the ray path, and γ is the angle between the ray and $-\nabla n$ (see Figure 1). Equation 6 may also be deduced from Fermat's principle, and so in a sense it is a further generalization of Snell's law for rays whose paths always lie in the same vertical plane. It follows from Figure 1 that

$$\sin \gamma = \cos (\theta - \psi)$$
$$= \cos \theta \cos \psi + \sin \theta \sin \psi$$

with

$$\cos \psi = -\frac{\partial n/\partial z}{|\nabla n|} \qquad \sin \psi = \frac{\partial n/\partial x}{|\nabla n|} \tag{7}$$

[2] The three-dimensional curvature formula applicable when lateral curvature exists is shown as equation 39 in the appendix.

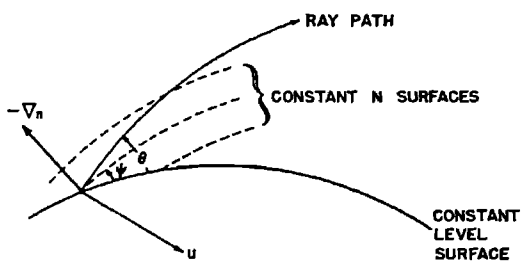

Fig. 1. Relationship of constant refractivity surfaces and ray geometry.

Here δz and δx are elements of distance measured vertically and horizontally, respectively. Hence, using $n - 1 = 10^{-6} \times N$, we may write (6) in the form

$$\frac{d\tau}{ds} = K = \frac{10^{-6}\left[-\dfrac{\partial N}{\partial z} \cos \theta + \dfrac{\partial N}{\partial x} \sin \theta\right]}{n} \tag{8}$$

In (7), ψ is the angle of elevation of the surfaces of constant N, and θ is defined just below (3) as the ray-elevation angle *relative to* the great circle through the ray segment.

Marshall and Gordon [1957] indicate that the contribution to the bending effect which results from the horizontal gradient can be significant along coastal paths and in frontal situations. The extent of a similar bending effect implicit in a radioclimatological model to be introduced in section 2 is investigated in this paper. Computation of the horizontal-gradient contribution is also performed (section 5) for the case of an extreme model having a horizontal gradient N which is everywhere ten times that of section 2.

As will be proved in the appendix, use of (8) instead of the three-dimensional curvature corresponding to the appropriate ray azimuth maximizes the ratio of the horizontal to vertical gradient contributions to bending. Thus (8) affords a useful simplification for computational estimates of horizontal bending effects associated with a *time-* and *space-smoothed refractivity distribution.* When small-scale turbulent irregularities in N are superimposed upon the large-scale distribution, the three-dimensional curvature equation (39) (see the appendix) must be employed to explain the distribution of 'ray-scarce' and 'ray-crossing' regions. Computer-integration techniques have been applied to this problem of propagation in irregular distributions of refractive index, notably by *Haselgrove* [1957] in England and by *Wong* [1960] and his coworkers in the United States. In this paper, we will perform computations of ray paths only for the regional-climatological model presented in section 2, that is to say, for a model which has been derived from synoptic data by considerable smoothing.

It will be noted in section 5 that, even if $\partial N/\partial x << \partial N/\partial z$, the latter derivative is strongly affected by the presence of a horizontal gradient. Thus for example, N may be expanded

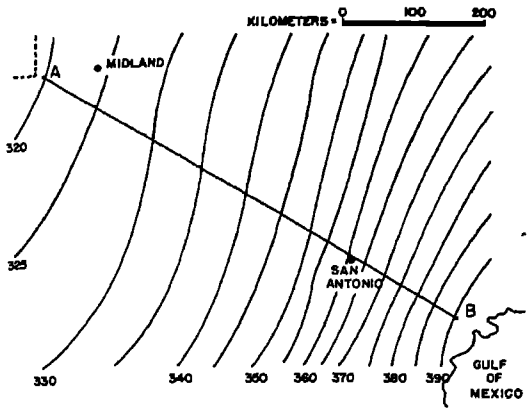

Fig. 2. The normal refractivity in central Texas during August, reduced to sea level [after *Bean and Thayer*, 1959].

about any initial point $(x_0, 0, z_0)$ in the form

$$\frac{\partial N}{\partial z} = \left(\frac{\partial N}{\partial z}\right)_0 + \left(\frac{\partial^2 N}{\partial z^2}\right)_0 (z - z_0) + \left[\frac{\partial}{\partial x}\left(\frac{\partial N}{\partial z}\right)\right]_0 (x - x_0) + \cdots \quad (9)$$

together with higher-order terms. The last term in (9) represents a significant contribution to $\partial N/\partial z$.

2. *The refractivity model.* The first step in developing the model was the fitting of a mean horizontal distribution of refractivity as a function of horizontal distance x from the transmitter site. The horizontal distribution was based upon regional radioclimatology published by *Bean and Thayer* [1959], depicting the mean sea-level refractivity N_0 at 1400 local time during the month of August. The mean N_0 distribution (see Figure 2) was prepared from 8-year average values of N_s, the surface refractivity, which were then reduced by Bean and Thayer to sea-level values N_0 by

$$N_0 = N_s \exp(0.1057h) \quad (10)$$

where h is the station altitude in kilometers above sea level. A hypothetical ray path AB was then drawn across the N_0 lines, essentially at right angles. Any ray initiated in the vertical plane through AB will then remain in this plane according to (6). Values of N_0 were extracted along AB, a distance of 705 km, and were fitted by polynomial functions of x, where x is the distance from the transmitter in meters. The best fit proved to be parabolic of the form

$$N_0 = D + Ex + Fx^2 \quad (11)$$

where $D = 320.4$ N units, $E = 2.801 \times 10^{-5}$ N units (meters)$^{-1}$, and $F = 1.025 \times 10^{-10}$ N unit (meters)$^{-2}$. The standard deviation of N_0 relative to its best fit (11) was 1.3 N units.

Next, the vertical distribution of refractivity was derived as a function of N_0. *Bean and Thayer* [1959] have devised model refractivity distributions of the form given in (1). The CRPL Exponential Atmosphere-1958 has the flexibility of allowing a climatological variation in the mean decay factor c_0. Simultaneous values of c_0 and N_s, after *Bean and Thayer* [1959], have been listed in Table 1 for $313.0 \leq N_s \leq 400.0$. It was possible to fit these paired variables by least squares, using a functional relationship of the form

$$c_0 = Ae^{bN_0} \quad (12)$$

The least-squares analysis gave the results $A = 0.05417$ (km)$^{-1}$ and $b = 3.089 \times 10^{-3}$ (N unit)$^{-1}$. The standard deviation in the mean c_0 values about the best-fit relation (12) was 0.00117 or about 0.5 per cent of the sample mean c_0 of Table 1. In the model adopted here, the best-fit relation (12) is assumed to be valid also for paired values of c_0 and N_0.

Combining (11) and (12), we have obtained a *regional model* which allows both N and $\partial N/\partial z$ to vary along the ray path as functions of x and z and yet retains consistency with earlier radioclimatological studies:

$$N = N_0 \exp[-Aze^{bN_0}], \qquad N_0 = D + Ex + Fx^2 \quad (13)$$

By differentiation of (13) with respect to x, it is readily shown that the level at which the

TABLE 1. Simultaneous Mean Values of N_s and c_0 after *Bean and Thayer* [1959], and c_0 Deduced by a Least-Squares Fit, Using Equation 12

N_s or N_0	c_0 (after Bean and Thayer), km^{-1}	c_0 by (12), km^{-1}
313.0	0.14386	0.14240
344.5	0.15680	0.15694
350.0	0.15934	0.15963
377.2	0.17323	0.17363
400.0	0.18672	0.18626

horizontal gradient of refractivity becomes zero from (13) may be determined from $z = (N_0 c_e b)^{-1}$, giving 7.0 km at point A and 4.6 km at point B. These levels compare reasonably well with the level 8 to 9 km, to which *Bean and Thayer* [1959] ascribe a minimum horizontal variability of N.

3. *The ray path.* Heretofore, curvature at any point on a ray path has been defined by $K = d\tau/ds$. Note that K signifies absolute curvature, which in cases of refraction within a vertical plane is the negative of the usual curvature defined in elementary texts on differential calculus. Relative curvature (with respect to the earth) may be defined by the equation

$$K_r = d\theta/ds \qquad (14)$$

where $d\theta$ is the change in ray direction relative to the (local) horizontal. From the geometry of Figure 3, it follows that[3]

$$d\theta = d\phi - d\tau \qquad (15)$$

[3] Equation 15 is similar to equation 8 of *Bean and Cahoon* [1959].

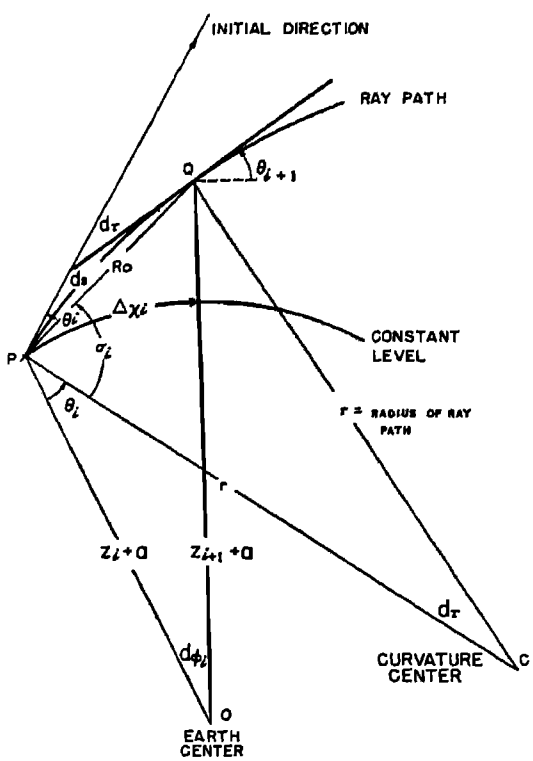

Fig. 3. Ray geometry of path tracing denoting the ith iteration.

where $d\phi$ is the *magnitude* of the angle at the earth's center subtended by the horizontal arc δx. We have, upon forming derivatives with respect to arc length s,

$$K_r = (\cos\theta)/(z + a) - K \qquad (16)$$

Knowing the values of $N = N(x, z)$ from the model (13), and the initial ray-elevation angle θ_0, we may determine K and K_r, respectively, by (8) and (16). Then by means of an iterative procedure, new values of θ_i, x_i, and z_i are computed with each successive iteration. Using finite differences applied to (6), we obtain the result

$$\theta_{i+1} = \theta_i + \Delta s[(\cos\theta_i)/(z_i + a) - K] \qquad (17)$$

where the subscript i denotes the ith iteration.

Next, z_{i+1} may be determined from the law of cosines applied to triangle OPQ (Figure 3) by means of the formula

$$z_{i+1} + a = [R_0^2 + (z_i + a)^2 - 2R_0(z_i + a)\cos(\sigma_i + \theta_i)]^{1/2} \qquad (18)$$

The side PQ of this triangle is the chord R_0, subtended by the arc Δs (Figure 3); it is given in terms of the radius of curvature r by

$$R_0 = 2r\sin(\Delta\tau/2) = 2/K\sin(K\Delta s/2) \qquad (19)$$

Note that the approximation $R_0 \approx \Delta s$ follows when the series expansion of $\sin(K\Delta s/2)$ is truncated at the first term. Using arc-length increments $\Delta s = 300$ meters, this approximation ($R_0 \approx \Delta s$) is valid for the model to an accuracy of 10^{-11} meter for each iteration.

The angle σ_i of (18) is one of the equal angles of the isosceles triangle CPQ, and its value in radians is obtained from

$$\sigma_i = \tfrac{1}{2}(\pi - \Delta\tau) \qquad (20)$$

Hence we have, upon expansion,

$$\begin{aligned}\cos(\sigma_i + \theta_i) &= \cos\left(\frac{\pi - \Delta\tau}{2}\right)\cos\theta_i \\ &\quad - \sin\theta_i \sin\left(\frac{\pi - \Delta\tau}{2}\right) \\ &= \sin\left(\frac{K\Delta s}{2}\right)\cos\theta_i \\ &\quad - \cos\left(\frac{K\Delta s}{2}\right)\sin\theta_i\end{aligned} \qquad (21)$$

Thus (18) becomes

$$z_{i+1} + a = \left\{(\Delta s)^2 + (z_i + a)^2 - 2\Delta s(z_i + a) \cdot \left[\frac{K\Delta s}{2} \cos \theta_i - \cos \frac{K\Delta s}{2} \sin \theta_i\right]\right\}^{1/2} \quad (22)$$

To determine successive values of Δx_i we must determine the corresponding angle $\Delta\phi_i$ subtended by the arc Δx_i at the earth's center (Figure 3); that is

$$\Delta x_i = (z_i + a)\Delta\phi_i \doteq (z_i + a) \sin \Delta\phi_i \quad (23)$$

where, in turn, by the law of sines applied to triangle OPQ,

$$\sin \Delta\phi_i = R_0 \sin (\sigma_i + \theta_i)/(z_{i+1} + a) \quad (24)$$

Hence, using a trigonometric identity for the expansion of sin $(\sigma_i + \theta_i)$, as well as (20) and (23), we obtain

$$\Delta x_i = (z_i + a)\Delta s \cdot \left[\frac{\cos (K\Delta s/2) \cos \theta_i + \sin (K\Delta s/2) \sin \theta_i}{z_{i+1} + a}\right] \quad (25)$$

The approximation $\Delta\phi_i = \sin \Delta\phi_i$ made in (23) is accurate to within 10^{-11} radian, and this approximation is virtually compensated in (25) by the approximation $R_0 \approx \Delta s$. From (25) we are then able to determine x_{i+1} by means of

$$x_{i+1} = x_i + \Delta x_i \quad (26)$$

The approximations of the form sin $(K\Delta s/2) \approx K\Delta s/2$ and sin $\Delta\phi_i \approx \Delta\phi_i$ used in (22) and (23) were made for convenience in using available programs of the CDC 1604 electronic computer. As indicated previously, for the small arc lengths involved, these approximations do not have any appreciable effect upon the accuracy of the ray path.

4. *Computational procedure.* Computations of the ray path were made with the equations outlined in the preceding sections. Iteration in arc-length steps of 300 meters along the path was performed using programs written by one of the authors for the CDC 1604 high-speed digital computer. An iterative procedure was devised utilizing the following steps.

(*a*) With the coordinates of the path x_i and z_i as horizontal distance along the earth and vertical height, respectively, point values of N_i, $(\partial N/\partial x)_i$, and $(\partial N/\partial z)_i$ were computed from (13). For example, $\partial N/\partial x$ and $\partial N/\partial z$ have the form

$$\partial N/\partial x = (E + 2Fx) \cdot (1 - N_0c_0bz) \exp (-c_0z) \quad (27)$$

$$\partial N/\partial z = -N_0c_0 \exp (-c_0z) \quad (28)$$

(*b*) Cos θ_i and sin θ_i were determined from known values of θ_i. Subroutines for these computations were already available in the program library of the computing center of the Naval Postgraduate School.

(*c*) The curvature $d\tau/ds$ was determined from (8).

(*d*) The values of z_{i+1}, x_{i+1}, and θ_{i+1} were computed from (22), (25), (26), and (17), respectively, in preparation for the next iteration and these values were stored in the computer memory.

(*e*) A printout was made at the end of each 9 km of path segment. The parameters printed were cumulative distance along the horizontal, cumulative vertical height, and path angle θ.

Ray paths were computed for initial angles of 0°, 0.5°, 1°, 3°, 5°, 15°, and 30° in the direction of increasing N_0, that is, from station A toward station B (Figure 2), constituting a range in N_0 from 320 to 390. The computations were also performed for the same initial angles but in the reverse direction, that is, for the rays emitted from a transmitter at point B.

5. *Comparisons.* The effect of the term $\partial N/\partial x$ of this model upon the value of K resulting from (8) was insignificant for all initial angles. The greatest height difference using the $\partial N/\partial x$ of this model resulted for the case of the initial angle of 0°, and even here there was less than 30 cm of height difference over the 705 km from B to A, in comparison with the case when $\partial N/\partial x$ was ignored. This is due primarily to the fact that $\partial N/\partial z$ is three orders of magnitude greater than $\partial N/\partial x$. At the surface, for example, the maximum vertical gradient is 7.050×10^{-2} N unit/m while the maximum horizontal gradient is 1.74×10^{-4} N unit/m. From (27) and (28), it is clear that the relative order of magnitude of $\partial N/\partial z$ to $\partial N/\partial x$ increases, even though the magnitudes of the derivatives simultaneously decrease with height.

TABLE 2. Effect of Extreme Horizontal Refractivity Gradient upon Path Height

(Ray projected from point B; $\theta_0 = 0.5°$.)				
Horizontal distance, km	231.75	365.72	548.79	705.00
Path height using model horizontal gradient, meters	3,232.10	10,493.64	22,586.29	37,488.72
Path height using extreme model, meters	3,232.40	10,494.57	22,587.51	37,490.25

When the value of $(\partial N/\partial x)_0$ in (8) was increased to five times its original value, the resulting height change was still less than 30 cm over the horizontal distance of 705 km from B to A. However, use of the extreme model in which the horizontal gradient is increased to ten times the model value caused the ray path to deviate from the model value by 157 cm, in the correct sense, over the same horizontal path (see Table 2). For the horizontal path B to A, $(\partial N/\partial x)_0$ is of opposite sign to $-(\partial N/\partial z)_0$, and by (8) the ray height increases as $|(\partial N/\partial x)_0|$ increases.

For low initial elevation angles, the vertical bending Δz_V is closely approximated by $\Delta z_V \approx z/4$, on the basis of the 4/3-earth model. Thus, from the results of Table 2, $\Delta z_V \approx 10$ km over the full horizontal path B to A. The corresponding horizontal bending Δz_H was 1.57 meters using the extreme model over the same path. Hence $\Delta z_H/\Delta z_V$ is about 10^{-4} under optimum horizontal bending conditions. Even for low elevation angles, the ray cannot be bent significantly out of the initial vertical plane for a ray whose azimuth direction differs from the horizontal gradient. This agrees with usual ray-tracing procedures. For rays whose initial elevation angles are large (30° or greater), the ratio $\Delta z_H/\Delta z_V$ is larger but the total ray bending is smaller, as is evident from Figure 4. In the latter range of angles, the rays are essentially straight. In any case, (8) reduces to (4) for the models considered here.

Figure 4 shows the path traced with '$N_0 = 320$

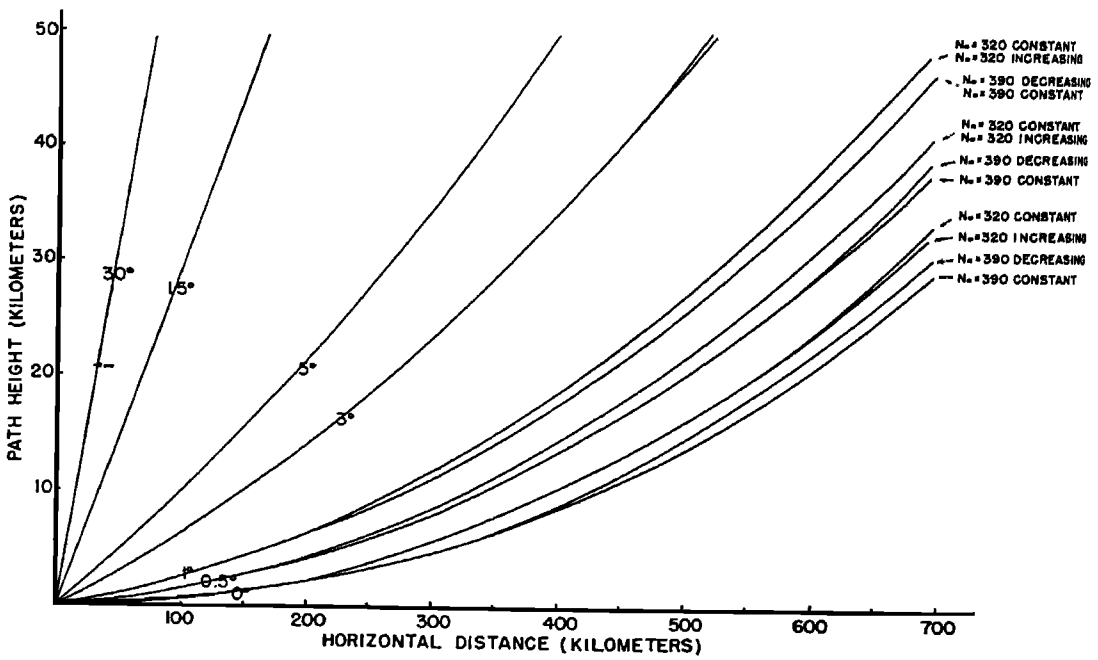

Fig. 4. Comparison of rays in a horizontally uniform atmosphere with those in a nonuniform atmosphere.

increasing' (from 320 to 390), that is, from point A to point B. For the same initial angle and initial elevation height, the rays have also been shown as they would have been transmitted from B to A. These are labeled '$N_0 = 390$ decreasing.'

Upon examination of Figure 4 the following major conclusions become evident.

(a) The ray paths corresponding to '$N_0 = 390$ decreasing' and '$N_0 = 320$ increasing' deviate more for small initial angles than for larger angles. For an initial elevation angle of 0.5°, the difference in height between the two rays was 1829.3 meters over the horizontal path of 705 km.

(b) The ray which initially experiences the maximum value of N_0, and therefore of $(\partial N/\partial z)_0$, is subjected to the greatest over-all bending, and it arrives at the end of the path at the lowest elevation. Thus, for example, the lower of the two rays mentioned in (a) above corresponds to '$N_0 = 390$ decreasing.'

(c) For small initial angles, the *ray paths of the horizontally homogeneous model deviate considerably* from those of the nonhomogeneous model mentioned in (a) and (b) above. For an initial elevation angle of 0.5° the ray path labeled '$N_0 = 390$ constant' gives an underestimate of the height of the corresponding nonhomogeneous model path ('$N_0 = 390$ decreasing') by about 594.5 meters over a horizontal distance of 705 km.

(d) Note from the considerations in (a) and (c) that as the initial elevation angle increases the corresponding curves become decreasingly separated in the vertical. For $\theta_0 = 1°$, only two curves are distinguishable, one for $N_0 = 390$ denoting both uniform and nonuniform horizontal distributions of refractivity and the other curve described similarly for $N_0 = 320$.

Conclusion (c) points up the concept of what might be called an *equivalent horizontally uniform* atmosphere. This atmosphere depends, however, upon two specifications pertaining to the ray path: (a) the horizontal path length over which the closest approximation is required and (b) the initial ray angle. As an illustration, specifications (a) and (b) were taken to be 320 km along the line B to A (Figure 2) and an initial ray angle of 0.5°. The computational procedure of section 4 was then used in testing the successive constant values of sea-level refractivity $N_0 = 390.0, \cdots, 381.0, 380.5, 380.0, 379.5, \cdots$.

The rms height error for *each horizontally uniform* model atmosphere identified by a particular $N_0 =$ constant was obtained using computed heights at horizontal increments of 9 km along the path. Errors were computed relative to the ray path '$N_0 = 390$ decreasing' (with $\theta_0 = 0.5°$). The minimum rms height error occurred for $N_0 = 380.0$, and comparative rms height errors for $N_0 = 380.5$, 380.0, and 379.5 over the 320-km path are 10.2 meters, 9.4 meters, and 10.7 meters, respectively.

The nature of the equivalent ray path determined by '$N_0 = 380.0$ constant' was such that it overshot the correct ray for approximately 4/5 of the path. The equivalent ray then crossed the correct path and proceeded beyond the crossover point at lower elevations. However, the magnitude of the errors associated with the last fifth of the equivalent ray path increased rapidly with increasing horizontal path length.

The equivalent horizontally homogeneous atmosphere is an idealization of a regional nonhomogeneous model, such as that depicted in Figure 2. Its usefulness lies in permitting simplification of the computational procedure of section 4 by choice of a mean value of N_0. In this simplified model, horizontal variations of N may be ignored.

6. *Conclusions.* The method of ray-path tracing employed here need not be confined to a regional climatological model of the type presented in section 2. It was convenient, however, to apply it to a model for which the distribution of refractivity could be described analytically as a function of the coordinates.

A possible application directed toward daily operational use may be found in the utilization of a modified CRPL Reference Atmosphere-1958 with actual synoptic values of $\Delta N_s = N_s - N_1$ to take account of surface ducts and other anomalous situations. At heights $z \geq 1$ km the decay factor c_e could be computed from the refractivity value $N_1 = N_1(x)$, at the 1-km level, rather than from the surface value N_s. This would involve the determination of a single synoptic parameter N_1 over a network of stations rather than a knowledge of the complete soundings over the network.

It would be of interest to apply the three-dimensional curvature equations, (37) and (38),

to the computational procedure outlined primarily in sections 3 and 4. The purpose of such a study is to determine representative sets of ray paths for a variety of initial conditions within a refractivity field of the type mentioned in the preceding paragraph. Since horizontal bending is excluded from a strongly smoothed refractivity field, it is desirable to retain as much as possible of the fine structure of the lowest kilometer of the field. Some experimentation is necessary to determine the arc-length increment appropriate to the character of the space perturbations.

Appendix

The three-dimensional curvature. To develop a ray-curvature formula of more general applicability than that of (8), we draw upon the ray-propagation formulas derived by *Wong* [1960], employing the Fermat least-time principle in an isotropic medium. His equations can be further simplified by the use of a moving trihedral x, y, z coordinate frame whose zx plane contains the ray segment at each element of the path. Furthermore, we will choose the x axis along the geocentric circle containing the horizontal projection of the ray segment at its true elevation z rather than at a standard reference level, as was done by Wong. With these modifications, it follows that

$$\frac{dy}{dx} = 0 \quad \text{and} \quad \frac{d}{dx} = \frac{1}{(1 + z/a)} \frac{d}{dX}$$

where X is used to denote one of Wong's standardized coordinates. Wong's equations in our notation therefore become

$$\frac{d^2z}{dx^2} = \left[1 + \left(\frac{dz}{dx}\right)^2\right]\left(\frac{1}{n}\frac{\partial n}{\partial z} + \frac{1}{a + z}\right) - \frac{dz}{dx}\left[1 + \left(\frac{dz}{dx}\right)^2\right]\left(\frac{1}{n}\frac{\partial n}{\partial x}\right) \tag{29}$$

$$\frac{d^2y}{dx^2} = \left[1 + \left(\frac{dz}{dx}\right)^2\right]\left(\frac{1}{n}\frac{\partial n}{\partial y}\right)$$

These two equations are related to the two components of curvature. Thus, if we write θ and ϵ as the ray-elevation and azimuth angles, respectively, we have $dz/dx = \tan\theta$ and $dy/dx = \tan\epsilon$, with $\epsilon = 0$ at any point of a ray segment. Differentiation with respect to x gives

$$d^2z/dx^2 = \sec^3\theta\, d\theta/ds \tag{30}$$

$$d^2y/dx^2 = d\epsilon/dx \tag{31}$$

From (30), (31), and (29) we obtain the components of relative curvature in the vertical plane and lateral to it, respectively.

$$\frac{d\theta}{ds} = K_r = \cos\theta\left(\frac{1}{n}\frac{\partial n}{\partial z} + \frac{1}{a + z}\right) - \sin\theta\left(\frac{1}{n}\frac{\partial n}{\partial x}\right) \tag{32}$$

$$\frac{d\epsilon}{dx} = \frac{d^2y}{dx^2} = \sec^2\theta\left(\frac{1}{n}\frac{\partial n}{\partial y}\right) = K_y' \tag{33}$$

K_r of (32) has already (section 3) been called the relative curvature and it is related to the absolute curvature in the vertical plane, K_{zz}, as K_r was related to K in (16). Thus we have

$$K_{zz} = \frac{\cos\theta}{a + z} - \frac{d\theta}{ds}$$

and from (32) it follows that

$$K_{zz} = -\frac{1}{n}\frac{\partial n}{\partial z}\cos\theta + \frac{1}{n}\frac{\partial n}{\partial x}\sin\theta \tag{34}$$

Likewise $d\epsilon/dx$ may be called the lateral curvature, and it has been symbolized by K_y' in (33).

Equations 33 and 34 constitute a system of relations which permit stepwise computation of the ray path under more general initial conditions than those considered in sections 3, 4, and 5. As mentioned previously (section 1), when the refractivity field has small-scale irregularities, the lateral bending term may be of some importance.

The unit tangent vector $\mathbf{t}$ at any point on the ray path may be written

$$\mathbf{t} = \mathbf{i}\cos\theta + \mathbf{k}\sin\theta \tag{35}$$

and upon differentiation with respect to arc length, we obtain

$$\mathbf{K} = \frac{d\mathbf{t}}{ds} = \left(\frac{\cos\theta}{a + z} - \frac{d\theta}{ds}\right) \cdot [\mathbf{i}\sin\theta - \mathbf{k}\cos\theta] + \mathbf{j}K_y'\cos^2\theta \tag{36}$$

where $K_y' = d^2y/dx^2$. The expression within the brackets is the unit normal vector (perpendicular to $\mathbf{t}$) lying in the zx plane, and it will be denoted by $\mathbf{u}_{zz} = \mathbf{i}\sin\theta - \mathbf{k}\cos\theta$. Thus by (34) and (36) we have

$$\mathbf{K} = \frac{1}{n}\left(-\cos\theta\,\frac{\partial n}{\partial z} + \sin\theta\,\frac{\partial n}{\partial x}\right)\mathbf{u}_{xz} + \mathbf{j}K_y'\cos^2\theta \qquad (37)$$

Let the y component of curvature $\mathbf{K}$ of (37) be denoted K_y. Since this component is related to K_y' of (33), it follows that

$$K_y = \left(\sec^2\theta\,\frac{1}{n}\frac{\partial n}{\partial y}\right)\cos^2\theta = \frac{1}{n}\frac{\partial n}{\partial y} \qquad (38)$$

It is convenient now to consider the vector curvature $\mathbf{K}$ in the form

$$\mathbf{K} = K_{xz}(\mathbf{i}\sin\theta - \mathbf{k}\cos\theta) + \mathbf{j}\frac{1}{n}\frac{\partial n}{\partial y} \qquad (39)$$

and simultaneously, in the equivalent form

$$\mathbf{K} = |\mathbf{K}|\,[\mathbf{i}\cos\phi_x + \mathbf{k}\cos\phi_z + \mathbf{j}\cos\phi_y] \qquad (40)$$

where ϕ_x, ϕ_y, and ϕ_z are the three direction angles made by the curvature vector with the local x, y, and z axes.

Comparison of (39) and (40), with K_z and $\cos\phi_z$ now considered to be positive,[4] leads to the results

$$\begin{aligned} K_z &= |\mathbf{K}|\cos\phi_z = K_{xz}\cos\theta \\ K_x &= |\mathbf{K}|\cos\phi_x = \pm K_{xz}\sin\theta \\ K_y &= |\mathbf{K}|\cos\phi_y \end{aligned} \qquad (41)$$

where the last of these is also equal to $(1/n)(\partial n/\partial y)$. The choice of sign to be used in connection with K_x in (41) is discussed below.

Let β be the azimuth direction, relative to the x axis, of the horizontal component of the curvature $\mathbf{K}$. Then the following projective relationships of solid geometry hold:

$$\begin{aligned} \cos\phi_x &= \sin\phi_z\cos\beta \\ \cos\phi_y &= -\sin\phi_z\sin\beta \end{aligned} \qquad (42)$$

The condition of perpendicularity of the unit tangent and curvature vectors leads to

$$\cos\theta\cos\phi_x - \sin\theta\cos\phi_z = 0 \qquad (43)$$

from which, using $\cos\phi_z$ from (42), we arrive at

$$\tan\theta = \cos\beta\tan\phi_z \qquad (44)$$

Using (41), (42), (43), and (44) in conjunction with (40), we obtain the curvature vector

$$\mathbf{K} = K_z[\mathbf{k} \pm \tan\theta(\mathbf{i} - \mathbf{j}\tan\beta)] \qquad (45)$$

The ratio of the magnitudes of the horizontal to the vertical components is therefore given by

$$|K_H|/K_z = \tan\theta\,|\sec\beta| \qquad (46)$$

Maximization of this ratio with respect to β is accomplished by differentiation, with the result

$$\frac{\partial}{\partial\beta}\left(\frac{|K_H|}{K_z}\right) = \tan\theta\,|\sec\beta\tan\beta|$$

The function $|K_H|/K_z$ has extreme values for $\beta = 0$ and $\beta = \pi$. According to (46) and (41) these two cases are characterized by the conditions $K_H = K_z$ and, in addition,

$$\begin{aligned} K_H &= K_{xz}\sin\theta \qquad \beta = 0 \\ K_H &= -K_{xz}\sin\theta \qquad \beta = \pi \end{aligned}$$

The first of these cases corresponds to the case in which $K_H = K_z$ has the same sign as $K_z = K_{xz}\cos\theta$, whereas in the second case the signs of K_H and K_z are opposite. Consequently, (39) reduces to (8), and the horizontal projection of the ray path is either parallel or opposite to the horizontal gradient vector $\nabla_H n$. In either case, the ratio $|K_H|/K_z$ is a maximum.

Acknowledgment. This work was supported in part by the Office of Naval Research.

References

Bean, B. R., and B. A. Cahoon, Effect of atmospheric horizontal inhomogeneity upon ray tracing, *J. Res. NBS, D, 63*, 287–292, 1959.

Bean, B. R., and G. D. Thayer, Models of the atmospheric radio refractivity index, *Proc. IRE, 47*, 740–755, 1959.

Haselgrove, J., Oblique ray paths in the ionosphere, *Proc. Phys. Soc. London, 70*, 653–662, 1957.

Kerr, D. E., *Propagation of Short Radio Waves*, pp. 44–45, McGraw-Hill Book Co., New York, 1951.

Marshall, J. S., and W. E. Gordon, Radiometeorology, in *Meteorological Research Reviews*, edited by H. Landsberg, *Meteorol. Monographs, 3*(14), 1957.

Smart, W. M., *Spherical Astronomy*, pp. 62–64, Cambridge University Press, London, 1931.

Wong, M. S., Ionospheric ray tracing with analog computer, in *Electromagnetic Wave Propagation*, edited by M. Desirant and J. L. Michiels, pp. 37–48, Academic Press, London, 1960.

(Manuscript received September 4, 1962; revised January 15, 1963.)

[4] This can be done by reflecting the z and y axes through 180 degrees.